Harjuoja, J., Kosola, A., Putkonen, M., and Niinistö, L., Atomic layer deposition and post-deposition annealing of $PbTiO_3$ thin films, Thin Solid Films 496 (2006) 346-352.

Available online at www.sciencedirect.com
SCIENCE DIRECT®
Thin Solid Films 496 (2006) 346 – 352
thin solid films
www.elsevier.com/locate/tsf

Atomic layer deposition and post-deposition annealing of $PbTiO_3$ thin films

Jenni Harjuoja *, Anne Kosola, Matti Putkonen, Lauri Niinistö

Laboratory of Inorganic and Analytical Chemistry, Helsinki University of Technology, P.O. Box 6100, FIN-02015 Espoo, Finland

Received 4 February 2005; received in revised form 24 August 2005; accepted 6 September 2005
Available online 29 September 2005

Abstract

Lead titanate thin films were deposited by atomic layer deposition on Si(100) using Ph_4Pb and Ti(O-*i*-Pr)$_4$ as metal precursors and O_3 and H_2O as oxygen sources. The influence of the Ti : Pb precursor pulsing ratio on the film growth, stoichiometry and quality was studied at two different temperatures, i.e. 250 and 300 °C. Uniform and stoichiometric films were obtained using a Ti : Pb precursor pulsing ratio of 1 : 10 at 250 °C or 1 : 28 at 300 °C. The as-deposited films were amorphous but the crystalline $PbTiO_3$ phase was obtained by rapid thermal annealing at 600–900 °C both in N_2 and O_2 ambient. Thin $PbTiO_3$ films were visually uniform and roughness values for as-deposited and annealed films were observed by atomic force microscopy.

PACS: 81.15.Gh; 77.84.-s; 68.55.Jk
Keywords: Lead titanate; Atomic layer deposition

1. Introduction

The family of lead titanate consists of a wide range of solid solutions, for example PZT (lead zirconate titanate), PLT (lead lanthanum titanate) and PLZT (lead lanthanum zirconate titanate). Adding dopants such as lanthanum and zirconium improves and optimizes the properties of lead titanate ($PbTiO_3$) for specific thin film applications, e.g. ferroelectric memories [1,2], pyroelectric infrared sensors [3–5], electro-optic devices [6–9] and insulator gates in metal–insulator–semiconductor diodes [10].

Perovskite-type $PbTiO_3$ has a high Curie temperature of 490 °C [11] and a relatively low permittivity compared to other lead titanates as well as a large pyroelectric coefficient. Lead titanate thin films have basically the same physical properties as the bulk material but in memory applications they exhibit low operating voltage and high switching speed [12].

Thin films of $PbTiO_3$ have been prepared by various chemical and physical methods, such as rf magnetron sputtering [13], pulsed laser ablation [10], sol–gel methods [14,15], spin-coating [16], chemical solution deposition [17] and, most recently, by a hybrid chemical method [18]. However, the most frequently used deposition method has been metal–organic chemical vapor deposition (MOCVD) and its variants such as laser-induced MOCVD [19], plasma-induced MOCVD [11,20,21] and ion beam-induced MOCVD [22]. In addition to the conventional CVD methods, the so-called improved MOCVD has been used to deposit *a*- and *c*-axis-oriented thin films. In this method, the metal precursor vapors have been alternately introduced into the reactor together with the oxygen source [23].

Except for a few attempts to use $TiCl_4$ [20] and titanium metoxide (Ti(OC_2H_5)$_4$) [22], titanium isopropoxide (Ti(O-*i*-Pr)$_4$) has been the Ti precursor of choice in MOCVD processes [15,17,24–32]. Typically, tetraethyl lead Pb(C_2H_5)$_4$ [23–28] or a β-diketonate complex Pb(thd)$_2$ (thd=2,2,6,6-tetramethyl-3,5-heptadione) [21,29–32] has been employed as the lead source. Both lead precursors have their drawbacks, however. Tetraethyl lead is highly toxic and, on the other hand, the decomposition behavior of Pb(thd)$_2$ is poorly understood [24]. The oxygen sources commonly used together with these lead precursors are oxygen [21,29,30], dinitrogen oxide (N_2O) [32] as well as a mixture of oxygen and ozone [23]. We have earlier used lead *tert*-butoxide complexes as ALD precursors to deposit PbS thin

* Corresponding author. Tel.: +358 4512589.
E-mail address: Jenni.Harjuoja@hut.fi (J. Harjuoja).

0040-6090/$ - see front matter © 2005 Elsevier B.V. All rights reserved.
doi:10.1016/j.tsf.2005.09.026

films [33]. In the present study it was found out, however, that $Pb(thd)_2$ is thermally significantly more stable than lead *tert*-butoxide complexes.

For practical applications the $PbTiO_3$ films have to meet some quality demands such as defect-free structure and low surface roughness [29]. Also the interface between the ferroelectric and the substrate is important. To avoid undesirable interfacial reactions during a semiconductor process, an as-low-as-possible deposition temperature is to be preferred. Atomic layer deposition (ALD), also referred to as atomic layer epitaxy or atomic layer CVD, is an advanced modification of the CVD process where the deposition temperatures are typically low. Unlike conventional CVD, ALD is based on surface-controlled reactions of precursors without any gas phase decomposition [34–37]. In an ALD process, the thin film growth is through its inherent surface control self-limiting but for a controlled deposition thermodynamically stable precursors are needed. The precursor pulses are alternately introduced onto the substrates, i.e. in the case of oxide materials the metal precursor and the oxygen precursor pulses are separated from each other by inert gas purging. Depositing ternary oxides is performed simply by alternately depositing two binary oxides and in an ideal ALD process the composition control and doping are straightforward and achieved by altering the precursor pulsing ratio. Consequently, it is important to understand the binary oxide processes before depositing ternary thin films.

Some ternary titanates such as $SrTiO_3$ [38–41], $BaTiO_3$ [42] and Bi–Ti–O [43] have previously been deposited by ALD. Before depositing by ALD the more complex titanate phases like PZT or PLZT, however, we have to understand the behavior, properties and deposition process of the parent compound viz. lead titanate. Unfortunately, atomic layer deposition of $PbTiO_3$ has not been reported so far and this fact prompted us to initiate the present investigation. In our previous study [44], tetraphenyl lead (Ph_4Pb) was found to be a thermally stable precursor producing uniform and impurity-free PbO_2 films with O_3 as oxygen source. In the present paper, we report the deposition of $PbTiO_3$ thin films by ALD at 250 and 300 °C using tetraphenyllead (Ph_4Pb) together with titanium isopropoxide (Ti(O-*i*-Pr)$_4$) for Pb and Ti precursors. The effect of Ti : Pb pulsing ratios on stoichiometry, crystallization and microstructure are discussed.

2. Experimental details

Film depositions were carried out in a commercial flow-type F-120 ALD reactor (ASM Microchemistry Ltd.). The pressure in the reactor during deposition was 200–300 Pa and two deposition temperatures 250 and 300 °C were explored. Tetraphenyl lead (Ph_4Pb, Aldrich Chem. Co., 97%) and titanium isopropoxide (Ti(O-*i*-Pr)$_4$, Aldrich Chem. Co., 97%) were used as precursors. Based on our previous studies [44,45] the Pb and Ti precursors were evaporated from open boats inside the reactor at 165 and 40°C, respectively. The reactants were alternately introduced into the reactor by using nitrogen as carrier and purging gas. High-purity nitrogen (>99.999%) was produced in a nitrogen generator (Nitrox UHPN 3000-1). Ozone generated from oxygen (>99.999%) in an ozone generator (Fischer model 502) and water vaporized in a cylinder kept at 30 °C were used as oxygen sources for Ph_4Pb and Ti(O-*i*-Pr)$_4$, respectively. The size of the Si(100) (Okmetic, Finland) substrates used was 5×10 cm^2.

At first the deposition processes of binary oxides were investigated in order to define the growth parameters for the ternary oxide process. The TiO_2 process parameters suggested by Ritala et al. [45] were slightly modified for the present reactor conditions used. For the lead precursor, a detailed study of the PbO_2 process was performed and is reported elsewhere [44]. Uniform thin films of $PbTiO_3$ were obtained when the reactant pulse durations were 1.5 and 0.6 s for Ph_4Pb and Ti(O-*i*-Pr)$_4$, respectively. Pulse duration for O_3 was 2 s and for H_2O 1 s. Purging times were between 1 and 2 s, depending on the preceding precursor pulsing lengths.

When depositing the ternary $PbTiO_3$ thin films, the ratio of binary oxide layers was altered by changing the relative number of the Ph_4Pb/O_3 and Ti(O-*i*-Pr)$_4$/H_2O pulses. The films were deposited by applying a certain number of lead oxide cycles followed by one titanium oxide cycle and then repeating that sequence. Typically the number of lead oxide cycles was varied between 5 and 50. The total number of PbO_2/TiO_2 layers was varied to obtain the desired film thickness.

Thicknesses of the deposited $PbTiO_3$ films were evaluated in a Hitachi U-2000 spectrometer using the wavelength region 190–1100 nm. After measuring reflectance spectra, film thicknesses were determined by using the fitting of the optical spectra as described by Ylilammi and Ranta-aho [46].

The Pb and Ti contents were measured using Philips PW 1480 X-ray fluorescence spectrometer equipped with a Rh X-ray tube [47]. Data analysis was performed with Uniquant 4.34 program, which utilizes the de Jongh Kappa model to calculate simultaneously the composition and mass thickness of an unknown sample [48]. Rutherford back scattering spectrometry (RBS) was used to verify the lead to titanium ratio obtained by the X-ray fluorescence (XRF) method. RBS measurements were carried out at the Accelerator Laboratory of the University of Helsinki. In these measurements, a 500 keV and a 1 MeV $^4He^+$ beam was used in order to determine the Ti/Pb ratio in deposited films.

The concentrations of possible impurities were measured by an ion-beam technique [49], viz. time-of-flight elastic recoil detection analysis (TOF-ERDA) for selected samples. TOF-ERDA measurements were carried out at the Accelerator Laboratory of the University of Helsinki. In this method, heavy ions are accelerated and projected into the sample [50]. When high-energy ions hit the sample, elastic collisions result and recoils of the sample atoms are measured. Timing gates and charged particle detector were utilized to determine recoil velocity and energy, respectively, which enabled mass separation. For these TOF-ERDA measurements, a 53 MeV $^{127}I^{10+}$ ion beam was used, obtained from a 5 MV tandem accelerator EGP-10-II. Samples were measured at 20° tilt and the recoils were detected at 20° with respect to the incoming beam.

The film crystallinity and its preferred orientation were studied by X-ray diffractometry (XRD, Philips MPD 1880) using Cu K_α radiation. Selected samples were annealed in a rapid thermal annealing (RTA) oven (PEO 601, ATV Technologie GmbH, Germany) in N_2 or O_2 (>99.999%) atmosphere at 500–900 °C for 10 min at atmospheric pressure. Heating rate of 20 °C/min and cooling rate of 25 °C/min were used. Surface morphologies of selected samples were studied with an atomic force microscope (AFM) AutoProbe CP (Park Scientific Instruments/Veeco) operated in the intermittent-contact mode using Ultralevers Si cantilevers with tip radius less or about 10 nm and cone angle 20°. Roughness was calculated as root-mean-square (rms) values.

3. Results and discussion

3.1. The deposition process and characterization of the films

When depositing ternary oxides the optimum growth temperature has to be chosen which is suitable for each binary oxide. With alkoxide precursors, like titanium isopropoxide, there is a risk that self-controlled ALD growth is destroyed by thermal decomposition of the precursor. Previous results have shown that when using Ti(O-*i*-Pr)$_4$ as a precursor in an ALD process, the temperature-independent TiO_2 growth rate can be obtained at temperatures between 150 and 250 °C [51]. However, also higher temperatures up to 325 °C have been successfully used to deposit TiO_2 [38,45,54]. In our earlier studies, a constant growth rate was obtained for PbO between 200 and 250 °C, but also at 300 °C the growth rate was independent of the pulse length and the films were uniform [44]. Therefore, we chose the reactor temperatures 250 and 300 °C for depositing the $PbTiO_3$ films. These temperatures were also chosen for further studies to deposit more complicated oxides PZT and PLT. Optimum growth temperature for ZrO_2 in ALD is around 275–400 °C depending on the precursor used [52] and for La_2O_3 is 225–275 °C [53].

When depositing oxides, the hydroxyl groups often terminate the surface after exposure to an oxygen source [54,55]. These hydroxyl groups then act as adsorption sites for the forthcoming metal precursor. According to Matero et al. [54], in the case of Ti(O-*i*-Pr)$_4$ the water dose has a significant effect on the growth rate. Also in our experiments the growth rate of

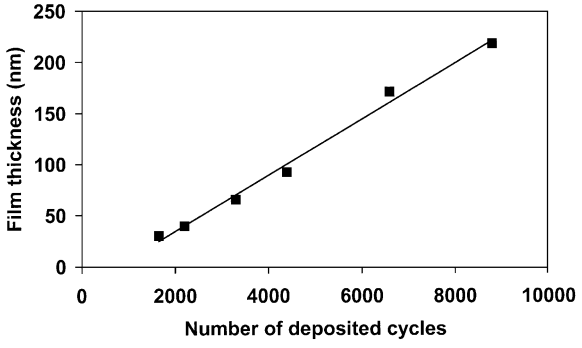

Fig. 1. Dependence of the $PbTiO_3$ film thickness as a function of the number of deposition cycles at 250 °C. Ti : Pb pulsing ratio has been 1 : 10.

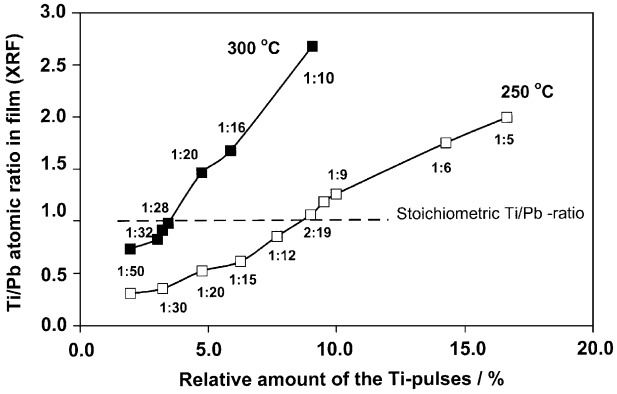

Fig. 2. Ti/Pb atomic ratio in $PbTiO_3$ films as a function of pulsing ratio of Ti(O-*i*-Pr)$_4$/H_2O–Ph_4Pb/O_3. Films were deposited at temperatures 250 and 300 °C. Pulsing ratio is expressed as a relative number of Ti(O-*i*-Pr)$_4$ pulses, calculated from the number of metal-containing precursors in one cycle by the formula: 100 × Ti(O-*i*-Pr)$_4$/(Ti(O-*i*-Pr)$_4$ + Ph_4Pb pulses).

TiO_2 at 250 °C increased from 0.30 to 0.60 Å per cycle when the water pulse was lengthened from 1 to 1.5 s. However, the lengthening of the water pulse did not change the growth rate at 300 °C, but the deposition rate of 0.44 Å/cycle was observed regardless of the H_2O pulse time. This could be explained by an increase of dehydroxylation rate leading to a constant growth rate independent of the H_2O pulse length [54].

The growth rate of PbO thin films was found to be 0.13 Å/cycle at 250 °C and 0.10 Å/cycle at 300 °C when using 1–1.5 s pulsing times for Ph_4Pb [44]. To obtain sufficient surface saturation, the pulse time of 1.5 s for Ph_4Pb was used when depositing $PbTiO_3$. The other pulsing times were 2 s for ozone, 0.6–0.8 s for titanium isopropoxide and 1 s for water.

Because lead oxide had a much lower growth rate than titanium dioxide, deposition of $PbTiO_3$ was initiated by varying the number of lead oxide cycles (Ph_4Pb/O_3) followed by one cycle of titanium dioxide (Ti(O-*i*-Pr)$_4$/H_2O). Under a constant deposition temperature and pulsing ratio, the film thickness of $PbTiO_3$ was found to be linearly dependent on the number of depositing cycles. Fig. 1 shows the results obtained with the Ti : Pb pulsing ratio of 1 : 10.

XRF measurements showed that the Ti/Pb atomic ratio in films was dependent on the relative number of the titanium pulses as seen in Fig. 2. The XRF results were calibrated by plotting the XRF Ti/Pb ratio against the Ti/Pb ratio measured by RBS. Results were in good internal agreement. When using the same pulsing ratio at 250 and 300 °C, the Ti/Pb ratio was higher in films deposited at higher temperature; this could, however, be explained with a higher deposition rate of PbO_2 at lower temperatures [44] and a higher deposition rate of TiO_2 at higher temperatures. Stoichiometric films were obtained at 250 °C with a Ti : Pb pulsing ratio of 1 : 10 and also at 300 °C with a pulsing ratio of 1 : 28. TOF-ERD analyses were performed for the film deposited onto Si(100) at 300 °C by a pulsing ratio of 1 : 32. Impurity levels were low and no other impurities than carbon and hydrogen were detected. Carbon content was less than 0.2% and hydrogen content was in the range of 0.1–0.5%.

In the present study, the relative growth rate of $PbTiO_3$ was found to be dependent not only on the pulsing ratio of

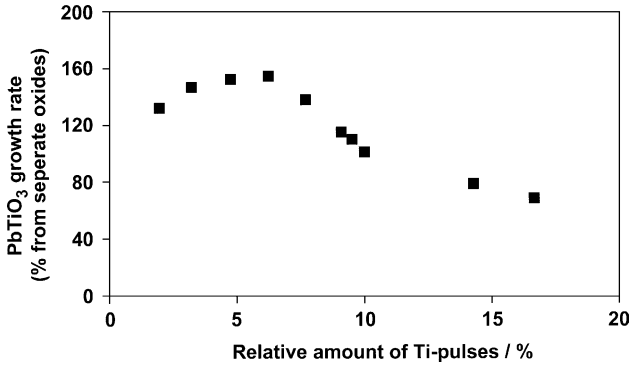

Fig. 3. $PbTiO_3$ growth rate compared with those for the separate TiO_2 and PbO processes. Films are deposited at 250 °C, the total number of lead cycles being about 6000.

precursors (Fig. 3) but also on the deposition temperature. In theory, a stoichiometric oxide ABO_3 can be obtained simply by alternately pulsing the two metal-containing precursors and an oxygen source and the growth rate of the ternary oxide can be predicted, as a first approximation, by summing up the growth rates of the constituent oxides. In practice, however, both assumptions often fail due to the different reactivities of the precursors [56,57]. The effects of surface chemistry usually cause changes in relative growth rates, which can be determined by comparing the observed film thickness with the theoretical thickness calculated from the growth rates of binary oxides. Previously the relative growth rate of $SrTiO_3$ was found to decrease when the relative number of Ti pulses was increased [38,39]. However, in the case of yttria-stabilised zirconia (YSZ) a slight increase in the relative growth rate has been observed when the relative number of yttrium pulses was increased [58]. In this study, maximum relative growth rates were obtained at 250 and 300 °C by using Ti : Pb pulsing ratios of 1 : 15 and 1 : 50, respectively, being 155% at 250 °C and 190% at 300 °C. At 250 °C the lowest relative growth rate was only 68% of the calculated value at a pulsing ratio of 1 : 5. In the case of high number of Ti pulses, a low deposition growth rate could be due either to lower number of surface sites available on the Ti–O surface for absorption of Ph_4Pb or to a different bonding mode of Ph_4Pb on the Ti–O surface as proposed previously by us in the case of other ternary oxides [38,56].

The surface morphologies of selected $PbTiO_3$ samples deposited at 250 °C were analysed by AFM. In our study, the as-deposited films were quite uniform but the rms values were unexpectedly high compared to the values obtained previously for the binary oxides PbO_2 [44] and TiO_2 [45]. The rms value for the as-deposited $PbTiO_3$ film with thickness of 210 nm was 23.8 nm (Fig. 4a). In the previous study [44], rms value of 4.3 nm was obtained for a 120-nm thick PbO_2 film deposited at 250 °C and 4.7 nm for a 90-nm thick film deposited at 300 °C, while TiO_2 thin film deposited from titanium isopropoxide and water at 300 °C had a rms value of 5.5 nm. Nevertheless, even higher rms values up to 25 nm have

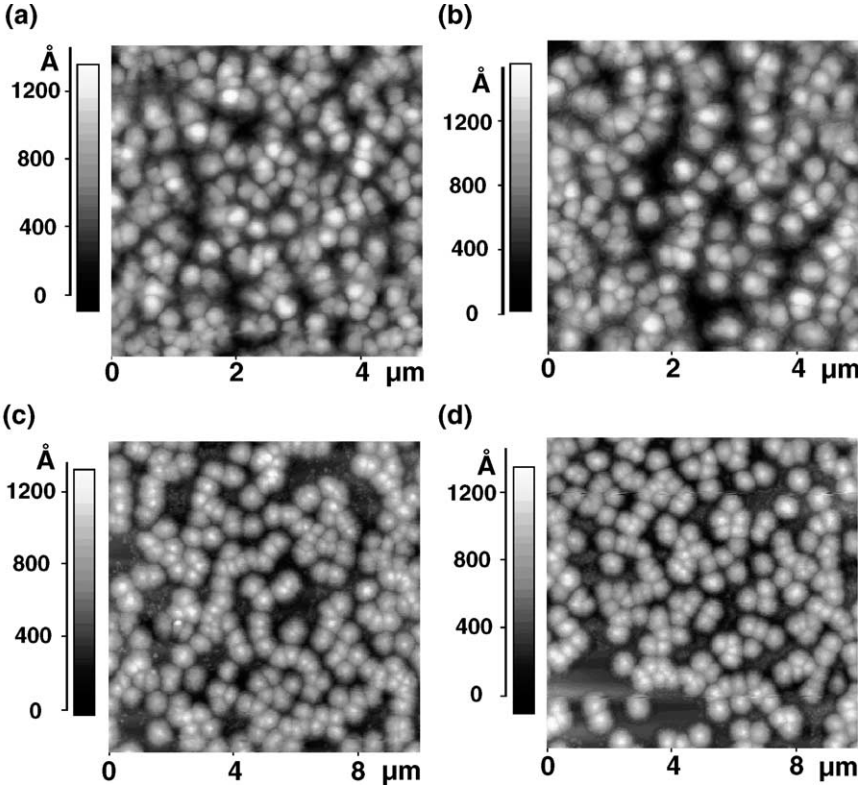

Fig. 4. AFM images of $PbTiO_3$ films deposited onto Si(100) substrate at 250 °C. Images (a) and (b) depict 210-nm thick films with image size of 5 × 5 µm. (a) As-deposited amorphous film, rms = 23.8 nm, and (b) film annealed at 600 °C in O_2 atmosphere for 10 min, rms = 27.4 nm. Images (c) and (d) show 150-nm thick films with image size of 10 × 10 µm: (c) film annealed at 600 °C in O_2 atmosphere for 10 min, rms = 23.0 nm and (d) film annealed at 600 °C in N_2 atmosphere for 10 min, rms = 24.5 nm. Note the different depth scales.

been obtained when titanium ethoxide ($Ti(OCH_2CH_3)_4$) has been used as precursor [59,60]. The rms value of $PbTiO_3$ slightly increased from 23.8 nm (Fig. 4a) measured from amorphous film to 27.4 nm (Fig. 4b) when the film was annealed at 600 °C in oxygen. For thinner 150 nm films the rms values depending on the annealing atmosphere were 23 and 24.5 nm (Fig. 4c and d).

3.2. The effect of annealing

Rapid thermal annealing (RTA) was used to study the crystallization process and preferred orientation of the $PbTiO_3$ films. The polycrystalline tetragonal perovskite $PbTiO_3$ phase [61] was detected by XRD when stoichiometric or lead-rich films deposited at 250 °C were annealed either in a nitrogen or oxygen atmosphere for 10 min in the temperature range of 600–900 °C. Annealing in oxygen turned out to be a more promising way to crystallize $PbTiO_3$, however, because the films annealed in nitrogen at 700–900 °C had a patchy appearance, while the films annealed in oxygen were smooth and shiny even after annealing at 900 °C. The change in film appearance may be an indication of a reaction between the $PbTiO_3$ film and the silicon substrate, which is also supported by the fact that at 1000 °C a new XRD peak was observed at $d=3.24$ Å, belonging most probably to the Pb_2SiO_4 phase [62]. Nevertheless, there were only minor differences in the surface roughness caused by the annealing atmosphere because rms values 23.0 and 24.5 nm were obtained for a 150-nm thick film in O_2 and in N_2, respectively (Fig. 4c and d). Adhesion of the films was tested by the tape test [63], but no peeling was observed regardless of the annealing temperature.

According to XRD, the films annealed at 500–550 °C did not contain the perovskite phase. Instead, a very broad peak at $d=3.01$ Å was observed in the stoichiometric films, probably belonging to the pyrochlore-type $Pb_2Ti_2O_6$ phase which is a metastable cubic phase and transforms to the perovskite structure upon heating at higher temperatures [64]. Thus, it can be concluded that the crystallization of ALD-processed $PbTiO_3$ thin films took place in the temperature range of 550–600 °C.

In addition to the perovskite phase, all films annealed at 600 °C showed also some XRD peaks, which could not be unambiguously identified due to their low intensities (Fig. 5). We suppose that these reflections belong to the monoclinic $PbTi_3O_7$ [65] and tetragonal PbO (litharge) phases, although the presence of orthorhombic PbO (massicot) and pyrochlore-type $Pb_2Ti_2O_6$ cannot be altogether ruled out. After annealing in oxygen, the relative intensities of these peaks were lower compared to samples annealed in nitrogen. These peaks were also present in stoichiometric films but only after annealing at higher temperatures. However, their relative intensities decreased with an increasing annealing temperature. Otherwise, the annealing temperature did not affect much the crystallinity of the $PbTiO_3$ phase. Interestingly, when lead-rich films with Ti/Pb ratios between 0.6–0.8 were annealed above 600 °C, only the reflections of the $PbTiO_3$ phase were detected. Thus, it seems that the presence of excess lead, probably in the form of amorphous lead oxide, somehow promotes the crystallization of $PbTiO_3$ phase. A similar effect has also been observed in the case of ALD-prepared $SrTiO_3$ films [38].

The effects of Ti/Pb atomic ratio and annealing temperature on the $PbTiO_3$ thin film formation and crystallization were studied in detail using oxygen atmosphere and an annealing time of 10 min. The results are summarized in Fig. 6. For the lead-rich and stoichiometric films (Ti/Pb atomic ratios of 0.61–0.99) deposited at 250 °C, the tetragonal perovskite phase was obtained by annealing at temperatures between 600 and 900 °C. In titanium-rich films (Ti/Pb 1.33), a monoclinic $PbTi_3O_7$ phase was detected by XRD after annealing at 600–800 °C. After annealing at 900 °C, however, cubic $PbTiO_3$ [66] and TiO_2 (rutile) [67] phases were observed. A film with even higher Ti/Pb ratio (1.98) was amorphous after annealing at 800 °C, but it crystallized at 900 °C showing the presence of $PbTi_3O_7$ and/or TiO_2 phases together with cubic $PbTiO_3$.

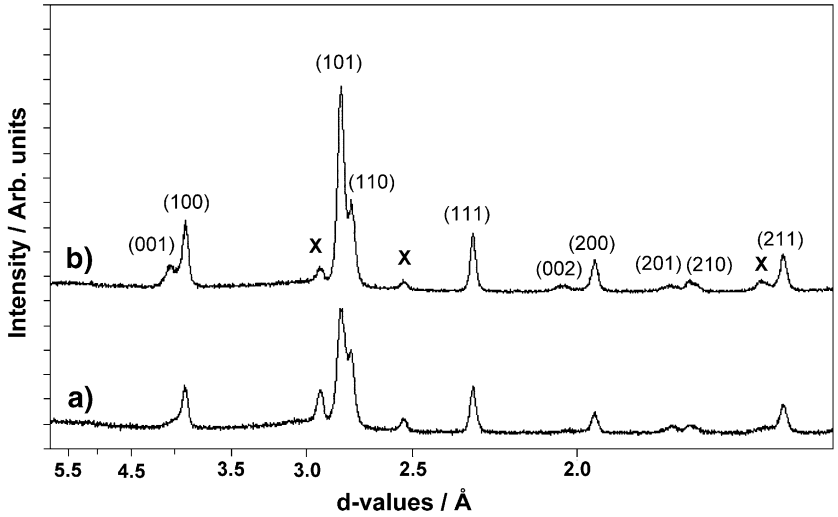

Fig. 5. XRD patterns of $PbTiO_3$ films (film thickness 154 nm, Ti/Pb ratio 0.95) deposited at 250 °C and annealed at 600 °C (a) in N_2 and (b) in O_2 atmosphere. The reflections marked with X represent an unidentified crystalline phase.

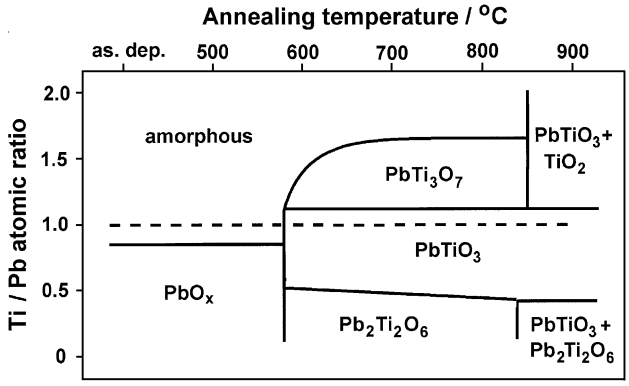

Fig. 6. The influence of stoichiometry and annealing temperature on the crystalline phases detected by XRD. The dashed line corresponds to the stoichiometric composition. The film deposition temperature was 250 °C.

Interestingly, the films deposited at 300 °C appeared to behave differently from the films deposited at 250 °C. Even an annealing temperature of 800 °C was not enough to crystallize the perovskite phase in oxygen atmosphere, unless the film contained a significant excess of lead (Ti/Pb 0.71). Even in this case the perovskite reflections were very weak and a lead oxide phase was also present. The annealing of the films with Ti/Pb ratio of 0.9 in O_2 at 800 °C resulted in a poorly crystalline lead oxide phase, while Ti-rich films remained amorphous. After annealing at 900 °C, the titanium-rich films showed the presence of the cubic $PbTiO_3$ phase but the Ti-rich monoclinic $PbTi_3O_7$ phase was detected, too. However, samples close to stoichiometric perovskite as well as the lead-rich films showed several additional XRD peaks of low intensity originating probably from various silicate phases.

Nevertheless, annealing in nitrogen seemed to be more favorable for the films deposited at 300 °C because in nitrogen the perovskite phase was obtained at annealing temperatures about 100 °C lower than those in oxygen. Still, 800 °C was needed to crystallize $PbTiO_3$. Taking into account the high annealing temperature needed and the poor degree of crystallization in the films deposited at 300 °C, the film deposition temperature 250 °C seems to be most suitable for depositing $PbTiO_3$ films by ALD from Ph_4Pb/O_3 and $Ti(O\text{-}i\text{-}Pr)_4/O_3$.

4. Conclusions

We have demonstrated the ALD growth of $PbTiO_3$ thin films on Si(100) substrate using Ph_4Pb/O_3 and $Ti(O\text{-}i\text{-}Pr)_4/H_2O$ as precursors. Furthermore, we have shown that stoichiometric films with excellent uniformity can be obtained already at 250 and 300 °C by a careful optimization of the Ti : Pb precursor pulsing ratios. The best quality films with stoichiometric Ti/Pb ratio were obtained at a deposition temperature of 250 °C using a Ti : Pb pulsing ratio of 1 : 10.

Under a constant deposition temperature and pulsing ratio, the film thickness of $PbTiO_3$ films was found to be linearly dependent on the number of deposition cycles in accordance with the ALD reaction mechanism. Films contained only small amounts of hydrogen and carbon impurities according to TOF-ERDA. As-deposited films were amorphous but crystalline $PbTiO_3$ thin films were obtained with RTA annealing treatment performed at 600 °C in both N_2 and O_2 atmospheres. As regard the smoothness, the rms values of as-deposited films were already quite high and the film roughness was slightly increased during annealing. It was found that the annealing atmosphere did not notably affect the rms values. However, the use of oxygen atmosphere was found to be a better option than nitrogen due to enhanced crystallinity and also because the appearance of the films annealed in nitrogen and the XRD data also indicated a reaction between the film and the silicon substrate.

Acknowledgements

The authors wish to thank Dr. Timo Sajavaara for TOF-ERD analysis and Dr. Eero Rauhala for the RBS measurement, both carried out at the Accelerator Laboratory of the University of Helsinki. We also wish to thank Mr. Raul Rammula at the University of Tartu for the AFM measurements. The authors are grateful to Professor Väinö Sammelselg, Institute of Physical Chemistry in the University of Tartu, for providing facilities for the AFM measurements. One of the authors (JH) wishes also to thank the support provided by the European Community Project (No. ICA1-1999-70086) as well as by the Jenny and Antti Wihuri Foundation.

References

[1] J.F. Scott, C.A. Paz de Araujo, Science 246 (1989) 1400.
[2] J. Carrano, C. Sudhama, V. Chikarmane, J. Lee, A. Tasch, W. Shepherd, N. Abt, IEEE Trans. Ultrason. 38 (1991) 690.
[3] R. Takayama, Y. Tomita, J. Asayama, K. Nomura, H. Ogawa, Sens. Actuators, A 21–23 (1990) 508.
[4] C. Shi, L. Meidong, L. Churong, Z. Yike, J. da Costa, Thin Solid Films 375 (2000) 288.
[5] L.M. Sheppard, Ceram. Bull. 71 (1992) 85.
[6] G.H. Haertling, Ferroelectrics 131 (1992) 1.
[7] D. Zhu, Q. Li, T. Lai, D. Mo, Y. Xu, J.D. Mackenzie, Thin Solid Films 313–314 (1998) 210.
[8] A. Boudrioua, J.C. Loulerque, E. Dogheche, D. Remiens, J. Appl. Phys. 85 (1999) 1780.
[9] M. Vellaikal, A.I. Kingon, Thin Solid Films 287 (1996) 139.
[10] S.G. Ghonge, E. Goo, R. Ramesh, Appl. Phys. Lett. 62 (1993) 1742.
[11] K. Nishida, G. Matuoka, M. Osada, M. Kakihana, T. Katoda, Appl. Surf. Sci. 216 (2003) 318.
[12] G.H. Haertling, J. Am. Ceram. Soc. 82 (1999) 797.
[13] Q. Zhao, Z.X. Fan, Z.S. Tang, X.J. Meng, J.L. Song, G.S. Wang, J.H. Chu, Surf. Coat. Technol. 160 (2002) 173.
[14] A. Li, D. Wu, C.Z. Ge, H. Wang, M. Wang, M. Wang, Z. Liu, N. Ming, Thin Solid Films 375 (2000) 220.
[15] D. Bao, X. Yao, N. Wakiya, K. Shinozaki, N. Mizutani, Mater. Sci. Eng., B 94 (2002) 269.
[16] Z. Kighelman, D. Damjanovic, M. Cantoni, N. Setter, J. Appl. Phys. 91 (2002) 1495.
[17] C.L. Sun, S.Y. Chen, M.Y. Yang, A. Chin, Mater. Chem. Phys. 78 (2002) 412.
[18] C. Ignacio, A.R. Soares, K. Yukimitu, J.C.S. Moraes, J.A. Malmonge, V.B. Nunes, S.I. Zanette, E.B. Araujo, Mater. Sci. Eng., A 346 (2003) 223.
[19] K. Tokita, F. Okada, J. Appl. Phys. 80 (1996) 7073.
[20] T. Mihara, S. Mochizuki, R. Makabe, Thin Solid Films 281–282 (1996) 457.
[21] Y.-B. Hahn, J.-W. Kim, C.-J. Youn, I.-S. Lee, J. Electron. Mater. 26 (1997) 1394.

[22] D. Leinen, A. Caballero, A. Fernandez, J.P. Espinos, A. Justo, A.R. Gonzalez-Elipe, J.M. Martin, B. Maurin-Perrier, Thin Solid Films 272 (1996) 99.
[23] T. Hirai, T. Goto, H. Matsuhashi, S. Tanimoto, Y. Tarui, Jpn. J. Appl. Phys. 32 (1993) 4078.
[24] C.-Y. Pan, D.-S. Tsai, L.-S. Hong, Mater. Chem. Phys. 70 (2001) 223.
[25] R.S. Batzer, B.M. Yen, D. Liu, H. Chen, H. Kubo, G.R. Bai, J. Appl. Phys. 80 (1996) 6235.
[26] L. Sun, Y.-F. Chen, T. Yu, N.-B. Ming, D.-S. Ding, Z.-H. Lu, Appl. Phys., A 63 (1996) 381.
[27] C. Byun, J.W. Jang, Y.-J. Cho, K.J. Lee, B.-W. Lee, Thin Solid Films 324 (1998) 94.
[28] L.S. Hong, C.C. Wei, Mater. Lett. 46 (2000) 149.
[29] Y.S. Yoon, J.H. Kim, W.K. Choi, J. Mater. Sci. 31 (1996) 5877.
[30] C.H. Wang, D.J. Won, D.J. Choi, J. Mater. Sci. 36 (2001) 815.
[31] Y.S. Yoon, W.N. Kang, S.S. Yom, T.W. Kim, M. Jung, H.J. Kim, T.H. Park, H.K. Na, Appl. Phys. Lett. 63 (1993) 1104.
[32] T.W. Kim, S.S. Yom, J. Phys. Chem. Solids 60 (1999) 935.
[33] E. Nykänen, J. Laine-Ylijoki, P. Soininen, L. Niinistö, M. Leskelä, L.G. Hubert-Pfalzgraf, J. Mater. Chem. 4 (1994) 1409.
[34] T. Suntola, A. Pakkala, S. Lindfors, US Patent 4,413,033, 1983.
[35] M. Ritala, M. Leskelä, in: H.S. Nalwa (Ed.), Handbook of Thin Film Materials, vol. 1, Academic Press, San Diego, 2002.
[36] L. Niinistö, J. Päiväsaari, J. Niinistö, M. Putkonen, M. Nieminen, Physica Status Solidi 201 (2004) 1443.
[37] M. Leskelä, M. Ritala, Thin Solid Films 409 (2002) 138.
[38] A. Kosola, M. Putkonen, L.-S. Johansson, L. Niinistö, Appl. Surf. Sci. 211 (2003) 102.
[39] M. Vehkamäki, T. Hänninen, M. Ritala, M. Leskelä, T. Sajavaara, E. Rauhala, J. Keinonen, Chem. Vap. Depos. 7 (2001) 75.
[40] D.-S. Kil, J.-M. Lee, J.-S. Roh, Vap. Chem. Depos. 8 (2002) 195.
[41] A. Rahtu, T. Hänninen, M. Ritala, J. Phys., IV 11 (2001) 923.
[42] M. Vehkamäki, T. Hatanpää, T. Hänninen, M. Ritala, M. Leskelä, Electrochem. Solid-State Lett. 2 (1999) 504.
[43] M. Schuisky, K. Kukli, M. Ritala, A. Hårsta, M. Leskelä, Chem. Vap. Depos. 6 (2000) 139.
[44] J. Harjuoja, M. Putkonen, L. Niinistö, Thin Solid Films (in press).
[45] M. Ritala, M. Leskelä, L. Niinistö, P. Haussalo, Chem. Mater. 5 (1993) 1174.
[46] M. Ylilammi, T. Ranta-aho, Thin Solid Films 232 (1993) 56.
[47] S. Lehto, L. Niinistö, I. Yliruokanen, Fresenius J. Anal. Chem. 346 (1993) 608.
[48] UniQuant Version 2 User Manual, Omega Data Systems, Neptunus 2, NL-5505 Velhoven, The Netherlands, 1995.
[49] M. Putkonen, T. Sajavaara, L. Niinistö, J. Keinonen, Anal. Bioanal. Chem. 382 (2005) 1791.
[50] K. Tokita, F. Okada, Nucl. Instrum. Methods Phys. Res., B 121 (1997) 408.
[51] J. Aarik, A. Aidla, T. Uustare, M. Ritala, M. Leskelä, Appl. Surf. Sci. 161 (2000) 385.
[52] M. Putkonen, L. Niinistö, J. Mater. Chem. 11 (2001) 3141.
[53] M. Nieminen, M. Putkonen, L. Niinistö, Appl. Surf. Sci. 174 (2001) 155.
[54] R. Matero, A. Rahtu, M. Ritala, M. Leskelä, T. Sajavaara, Thin Solid Films 368 (2000) 1.
[55] S. Haukka, E.-L. Lakomaa, T. Suntola, Stud. Surf. Sci. Catal. 120 (1998) 715.
[56] M. Nieminen, T. Sajavaara, E. Rauhala, M. Putkonen, L. Niinistö, J. Mater. Chem. 11 (2001) 2340.
[57] M. Nieminen, S. Lehto, L. Niinistö, J. Mater. Chem. 11 (2001) 3148.
[58] M. Putkonen, T. Sajavaara, J. Niinistö, L.-S. Johansson, L. Niinistö, J. Mater. Chem. 12 (2002) 1.
[59] J. Aarik, A. Aidla, V. Sammelselg, T. Uustare, M. Ritala, M. Leskelä, Thin Solid Films 370 (2000) 163–172.
[60] J. Aarik, S. Karlis, H. Mändar, T. Uustare, V. Sammelselg, Appl. Surf. Sci. 181 (2001) 339.
[61] Powder diffraction file, Joint Committee on Powder Diffraction Standards, Card 6-452.
[62] Powder diffraction file, Joint Committee on Powder Diffraction Standards, Card 30-724.
[63] B. Chapman, J. Vac. Sci. Technol. 11 (1974) 106.
[64] F.W. Martin, Phys. Chem. Glasses 6 (1965) 143.
[65] Powder diffraction file, Joint Committee on Powder Diffraction Standards, Card 21-949.
[66] Powder diffraction file, Joint Committee on Powder Diffraction Standards, Card 40-99.
[67] Powder diffraction file, Joint Committee on Powder Diffraction Standards, Card 21-1276.